



Article

Cite this article: Voermans JJ, Xu X, Babanin AV (2022). Validity of the wave stationarity assumption on estimates of wave attenuation in sea ice: toward a method for wave–ice attenuation observations at global scales. *Journal of Glaciology* 1–8. <https://doi.org/10.1017/jog.2022.99>

Received: 9 July 2022

Revised: 5 October 2022

Accepted: 7 October 2022

Keywords:

Atmosphere/ice/ocean interactions; sea ice; sea-ice dynamics

Author for correspondence:

Joey J. Voermans,

E-mail: jvoermans@unimelb.edu.au

Validity of the wave stationarity assumption on estimates of wave attenuation in sea ice: toward a method for wave–ice attenuation observations at global scales

Joey J. Voermans , Xingkun Xu and Alexander V. Babanin

Department of Infrastructure Engineering, University of Melbourne, Melbourne, Australia

Abstract

In situ observations of wave attenuation by sea ice are required to develop and validate wave–ice interaction parameterizations in coupled wave models. To estimate ice-induced wave attenuation in the field, the wave field is typically assumed to be stationary. In this study we investigate the validity of this assumption by creating a synthetic wave field in sea ice for different attenuation rates. We observe that errors in estimates of the wave attenuation rates are largest when attenuation rates are small or temporal averaging periods are short. Moreover, the adoption of the wave stationarity assumption can lead to negative estimates of the instantaneous wave attenuation rate. These apparent negative values should therefore not be attributed to wave growth or erroneous measurements a priori. Surprisingly, we observe that the validity of the wave stationarity assumption is irrelevant to the accuracy of estimates of wave attenuation rates as long as the temporal averaging period is taken sufficiently long. This may provide opportunities in using satellite-derived products to estimate wave attenuation rates in sea ice at global scales.

Introduction

Waves play a critical role in the coupled air–sea system and the mechanisms governing its dynamics thus require accurate representation in forecasting models. One of these dynamical impacts is the attenuation of wave energy by sea ice (Shen, 2019; Squire, 2020).

Many processes have been identified that contribute to the attenuation of wave energy in sea ice and are typically categorized as either a conservative, such as wave scattering (Kohout and Meylan, 2008; Montiel and others, 2016), or non-conservative process, such as the dissipation of energy by ice–floe collisions (Herman and others, 2019; Rabault and others, 2019; Løken and others, 2021), under-ice friction (Kohout and others, 2011; Voermans and others, 2019), overwash (Nelli and others, 2020) and viscous properties of the sea ice (Weber, 1987; Wang and Shen, 2010). Some of these processes and derived models have been developed, tested and calibrated through carefully designed laboratory experiments (e.g. Toffoli and others, 2015; Sree and others, 2018; Sutherland and others, 2019), and since implemented in operational wave forecasting models. However, a major concern is that most of these theories and models struggle to replicate observed attenuation trends from the field (Rogers and others, 2021). Thus, while there is theoretical and experimental support that each of these processes contribute to the attenuation of wave energy in sea ice, consensus is yet to be reached on the practical significance of each of these processes in the field and, importantly, under what environmental conditions these processes play a relevant role.

The most likely source of the discrepancy between theory and field observations is that sea ice is highly inhomogeneous (e.g. Shen, 2019), dynamic and changes rapidly in time due to, for instance, sea-ice break-up (e.g. Voermans and others, 2020). These inhomogeneities are difficult to capture consistently, both theoretically and numerically, and are near impossible to be mimicked and thus study at laboratory scales, leaving unanswered questions regarding the significance of the theories and models in the framework of field conditions. However, a secondary but often forgotten potential source of discrepancy between models and field observations are the methodological uncertainties and biases that lead to (often unspecified) errors in the field observations. An example of such a bias is the spurious rollover phenomenon identified by Thomson and others (2021), who showed that instrument noise introduces a negative bias in observations of wave attenuation at high frequencies. Other uncertainties may be introduced through the adoption of assumptions in estimating wave attenuation in sea ice from field observations, including assumptions on the directional distribution of wave energy, wind-input and wave field stationarity. Most of these assumptions remain unverified, simply because they are difficult to verify. In this study, however, we will look at the influence of one of these assumptions on field observations of wave attenuation in sea ice: the wave stationarity assumption.

Wave stationarity assumption

It is common practice to approximate the decay of wave energy as an exponential function with distance into the sea ice (e.g. Wadhams and others, 1988):

$$E(f, x) = E(f, 0) \exp(-\alpha x) \quad (1)$$

where $E(f, x)$ is the spectral energy density, f is the wave frequency and x is the distance from the ice edge. The wave attenuation coefficient α is the traditional focus of wave–ice interaction studies, and a variety of parameterizations have been proposed (the reader is referred to Squire (2020) and Rogers and others (2021) for an overview of the different parameterizations).

Following Eqn (1), estimating the wave attenuation rate in sea ice is, in principle, straightforward and is typically done by deploying two motion-sensing instruments (such as wave–ice buoys, e.g. Rabault and others, 2022) a distance x apart on the ice to measure $E(f, 0)$ and $E(f, x)$:

$$\alpha = \frac{-\ln(E(f, x)/E(f, 0))}{x} \quad (2)$$

Here, x may vary between tens of meters (such as for landfast ice, e.g. Sutherland and Rabault, 2016) up to as much as a hundred kilometers (Cheng and others, 2017).

As it takes time for wave energy to travel from the first to the second instrument, the wave energy at $E(f, x)$ needs to be measured, strictly speaking, somewhat later than at $E(f, 0)$ to obtain α . However, given the complexities of performing in situ experiments on sea ice and the relatively short travel times to cover distance x (e.g. the energy of a 7 s period wave takes about half an hour to travel a distance of 10 km), general practice is to measure the surface elevation at both locations at the same time. That is, we assume the incoming wave energy over this time period to be approximately constant, i.e. stationary. By assuming wave field stationarity, an error of ΔE is made in our measurements of wave energy at x , specified by the time shift $\Delta t = x/c_g$, where c_g is the wave group velocity.

To understand the significance of this error ΔE on observations of α , consider the case where the waves approaching the sea ice are growing, such that the wave energy at the ice edge momentarily increases in time. By measuring the wave energy at $x_1 = 0$ and $x_2 = x$ at the same time, where $x > 0$ is an arbitrary point, the wave energy $E(f, x)$ will be underestimated by:

$$\Delta E \approx -\frac{dE(f)}{dt} \Delta t = -\frac{dE(f)}{dt} \frac{x}{c_g} \quad (3)$$

This then makes it appear as if more wave energy was attenuated by the ice over distance x , leading to an overestimation of α by:

$$\Delta \alpha = \frac{-\ln(E/E_0)}{x} + \frac{\ln((E + \Delta E)/E_0)}{x} \quad (4)$$

While ΔE increases linearly with x (Eqn (3)), we note that, somewhat surprisingly, the error $\Delta \alpha$ is independent of x . This can be shown by taking the linear approximation of $\Delta \alpha(\Delta t)$ around $\Delta t = 0$, giving:

$$\Delta \alpha = -\frac{dE/dt}{Ec_g} \quad (5)$$

While independent of x , it also suggests that the error $\Delta \alpha$ is frequency dependent and varies with the properties of the wave field (or wave climate).

In this study, we will investigate the impact of the wave field stationarity assumption on estimates of wave attenuation in sea ice. The aim is to inform on the errors and uncertainties associated with the stationarity assumption to improve the analysis of wave attenuation data in future measurement campaigns. To

do so, we will rely largely on the validity of Eqn (1), which remains a topic of discussion to date (e.g. Squire, 2018; Herman, 2021). However, such a discussion is outside the scope of this study. In the process of evaluating the impact of the wave field stationarity assumption with very large Δt , we noticed a surprising result that may provide significant opportunities to derive estimates of wave attenuation by sea ice at large spatial scales using satellite-derived wave products.

Methods

Continuous observations of the wave field along a vast distance in the MIZ are required to assess the impact of the wave field stationarity assumption on estimates of wave attenuation. Because such an experimental field dataset is not available, we will generate a synthetic wave record instead. In doing so, we have to rely on the critical assumption that wave energy decays exponentially into the ice cover, i.e. Eqn (1) is deemed valid.

To characterize the incoming wave field $E(f, 0)$ we used wave hindcast data from ERA5 reanalysis. An energetic site in the Southern Ocean was chosen (51° S latitude and 127° E longitude) for the duration of 1 year (January–December 2020) with a data time interval of 1 h. The significant wave height H_s during this period varied between 2 and 10 m, with a median ~4 m. As the error $\Delta \alpha$ is independent of x (Eqn (5)), the results presented in this study do not rely on the severity of the incoming wave field $E(f, 0)$ and any other site could have been chosen. We verified this through comparison with data covering a milder sea state with a median H_s of 2.4 m (not shown here). We note that by considering a 1-D wave spectrum only, we are implicitly assuming that the wave field is unidirectional. Lastly, for the wave attenuation rate, we impose a wide range of $\alpha \in [10^{-7}, 10^{-2}]$, and do so for each wave frequency. We note that such values may be much larger or smaller than one may encounter for a given wave period in the field. As we predefine the values of α here, we refer to these as the ‘theoretical’ values with symbol α_{th} .

With definitions for α_{th} and the input wave energy $E(f, 0)$, the wave field $E(f, x)$ can be determined using Eqn (2) by considering the duration of wave energy propagation over the distance x , i.e. the time series at x will appear shifted in time. For c_g we use the open water dispersion relationship, which serves as a reasonable approximation of c_g in most ice conditions (we briefly come back to this assumption later on). Then, a time series of $\alpha(f)$ can be determined from $E(f, x)$, and an estimate of α can be derived by taking the time averaged value $\bar{\alpha}$ over an averaging period τ . Initially, we keep $\Delta t = x/c_g$ as is common for field experiments. Then, we will examine the impact of $\Delta t \gg x/c_g$ on estimates of α .

In addition to using ERA5 reanalysis data for the wave energy input, we have also examined in situ wave data from a wave buoy that was drifting in the Southern Ocean (Spotter, Sofar Ocean Technologies). The buoy drifted between 47° S and 49° S latitude and from 142° E to 159° E longitude over a period of ~2 months (28 April 2021–22 June 2021). The buoy measured a H_s between 2 and 9 m, with a median of 4 m, and spectral information was transmitted every hour (comparable wave field statistics as the ERA5 dataset used here). As the outcomes of our study are broadly comparable for the ERA5 and wave buoy datasets, we will only show the results of the ERA5 reanalysis dataset here. Nevertheless, there are some differences due to the ERA5 reanalysis data being smoother at timescales of the order of hours compared to the wave buoy data. Such differences are expected to be a combination of noise in the wave buoy data and the inability of numerical models to solve for such short timescale variability. Specifically, the wave field may not be perfectly stationary over the 0.5–1 h period from which the spectral data are derived, a variability that may be measured by the wave buoys, but will

not be simulated by the numerical models. It is this variability that causes $\Delta\alpha$ to be weakly dependent with x for the wave buoy observations. Readers interested in the impact of the wave stationarity assumption for the wave buoy data are referred to Figure S1, which compares the error in α for both datasets.

Results and discussion

An example time series of α is shown in Fig. 1 for a 7 s period wave with $\alpha_{th} = 1 \times 10^{-6}$ and $\alpha_{th} = 1 \times 10^{-4}$ with a measurement separation distance of $x = 10$ km. The estimated instantaneous attenuation rate α fluctuates around the theoretical value α_{th} when the duration of wave propagation over distance x is not taken into consideration (i.e. $\Delta t = x/c_g$). While the magnitude of the fluctuations for this wave condition are modest for the high α -case, they appear to be significant for the low α -case. Moreover, episodes of apparent negative attenuation rates can be retrieved when disregarding the lag in wave arrival time at the second measurement point (e.g. Fig. 1a). This may also, in part, explain the negative attenuation rates observed by Kodaira and others (2021) in grease ice who found large scatter of α ranging from positive to negative values for $T \geq 5$ s. As the mean of the 2 week time series shown in Fig. 1 are close to the theoretical values (i.e. 2% for the example in Fig. 1a and <0.1% for the example in Fig. 1b), the removal of apparent negative values of the estimated attenuation rates may not be disregarded a priori and should be carefully considered when evaluating estimates of α . For example, if negative values of α in Fig. 1a would be considered erroneous and were to be removed, $\bar{\alpha}$ would be significantly overestimated by $\bar{\alpha}/\alpha_{th} \approx 3.1$. We note, however, that the impact of apparent negative observations of α tends to be restricted to $\alpha_{th} < 10^{-5}$ (see Fig. S2).

In Fig. 2 the 95% confidence interval of the normalized error $(\bar{\alpha} - \alpha_{th})/\alpha_{th}$ is shown for a wide range of α_{th} , wave periods T , and for four different averaging periods τ . In color, several trends of $\alpha(T)$ are shown as derived from field observations by Hošeková

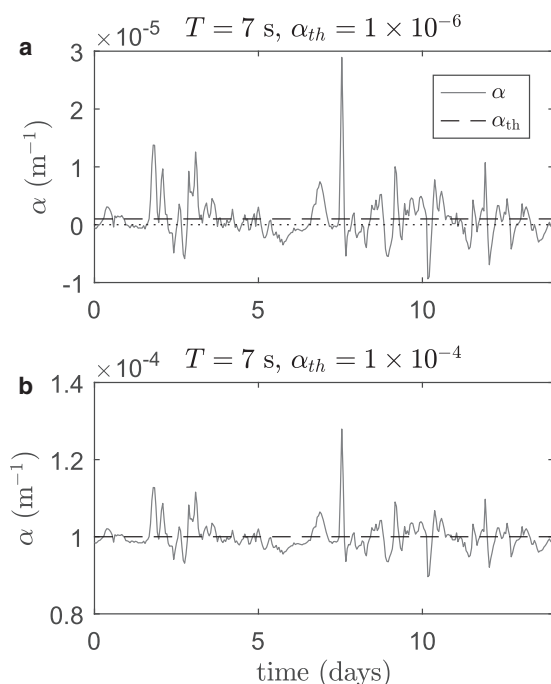


Fig. 1. Comparison of the estimated attenuation rate α when adopting the stationarity assumption (i.e. $\Delta t = x/c_g$, solid line) against the theoretical attenuation rate α_{th} (dashed line) for (a) $\alpha_{th} = 1 \times 10^{-6}$ and (b) $\alpha_{th} = 1 \times 10^{-4}$. For both cases, the wave period is $T = 7$ s and the measurement separation distance is 10 km.

and others (2020), Kodaira and others (2021), Li and others (2017), Meylan and others (2014), Rogers and others (2021), Thomson and others (2018) and Voermans and others (2021). We note that this is just a selection of in situ wave attenuation observations available, and are used to put the results into perspective of field observations of α . We also note that Rogers and others (2021) produced two primary observational trends from their dataset (see their Fig. 8), both of which are shown here. Figure 2a shows the error for instantaneous observations of α with $\Delta t = x/c_g$. Errors are largest for small α_{th} , typically observed for longer waves and/or waves in unconsolidated sea ice. Instantaneous errors can be as large as a factor of 10 of their true value. Errors reduce significantly when the observations of α are averaged over longer periods of time. For example, for $T = 10$ s and $\alpha_{th} = 1 \times 10^{-5}$ the error reduces from 46, 21, 4 to 1%, for $\tau = 1$ h, 1 d, 7 d to 28 d, respectively. However, although an increase in τ can greatly reduce uncertainties in $\bar{\alpha}$, this does require the ice conditions to remain constant over this measurement period. While the anticipated errors may be of significance for the low-frequency range in the observed trends of Rogers and others (2021), it is noteworthy that the derivation of α by Rogers and others (2021) is based on model-data inversion, and thus does not rely on the wave stationarity assumption.

As the open water dispersion relation may not be valid for very short waves and under certain ice conditions, such as consolidated sea ice, Figs 2a, b are replicated by using the dispersion relation in sea ice as derived by Squire and Allan (1980) (see Fig. S3). For this, a Young's modulus of 3 GPa and ice thickness of 0.5 m are taken as an example. The impact is largely constraint to the small wave periods which propagate faster in sea ice compared to open water, leading to a decrease in the observed error (e.g. Eqn (5)).

In Fig. 3a the distribution of the error $(\alpha - \alpha_{th})/\alpha_{th}$ is shown. From this we can see indeed that the error will approach 0 when the averaging period increases as the mean of the distributions are 0. This also puts forward two competing actors on the magnitude of the error in α : increases in Δt increases the error, whereas increases in τ reduces it. We now consider the case where two instruments deployed on the ice do not measure at the same time but with a time offset t_0 , i.e. $\Delta t = x/c_g + t_0$. As the autocorrelation timescale of the wave energy reaches 0 at ~ 5 –7 d for the dataset used here (not shown), the observed error increases with an increase of t_0 up to $t_0 \approx 5$ –7 d after which the error remains approximately constant. At this time offset, the distribution of the error seems to have approached a normal distribution with its mean at 0 (Fig. 3b). This would imply that the accuracy of α for very large $\Delta t \approx t_0 \gg 0$ is then simply determined by the duration of τ (or the number of random samples) necessary to achieve the required accuracy.

In Fig. 4 the 95% confidence interval of the error $(\bar{\alpha} - \alpha_{th})/\alpha_{th}$ is shown for various time offsets t_0 and averaging periods τ . As the autocorrelation timescale is ~ 7 d, increasing t_0 further does not considerably change the error. We note that introducing the time offset t_0 means that the error $\Delta\alpha$ is now dependent on x . Comparing Figs 2 and 4, the error made for instantaneous estimates of α when $t_0 = 0$ (Fig. 2a) is similar in magnitude as measuring α over a period of 1 d with an offset of $t_0 = 1$ h (Fig. 4a), or an averaging period of $\tau = 4$ weeks with a time offset of $t_0 = 1$ d (Fig. 4e). While it may seem unusual from a design perspective of in situ experiments to introduce a time offset in estimating α , it may, however, provide major opportunities in deriving observations of wave attenuation rates in sea ice using satellite observations (Stopa and others, 2016; Horvat and others, 2020; Brouwer and others, 2022) as satellite observations have a high spatial resolution but often a poor temporal resolution. If possible, this may then provide access to wave attenuation observations at a global reach, rather than local as with in situ experiments.

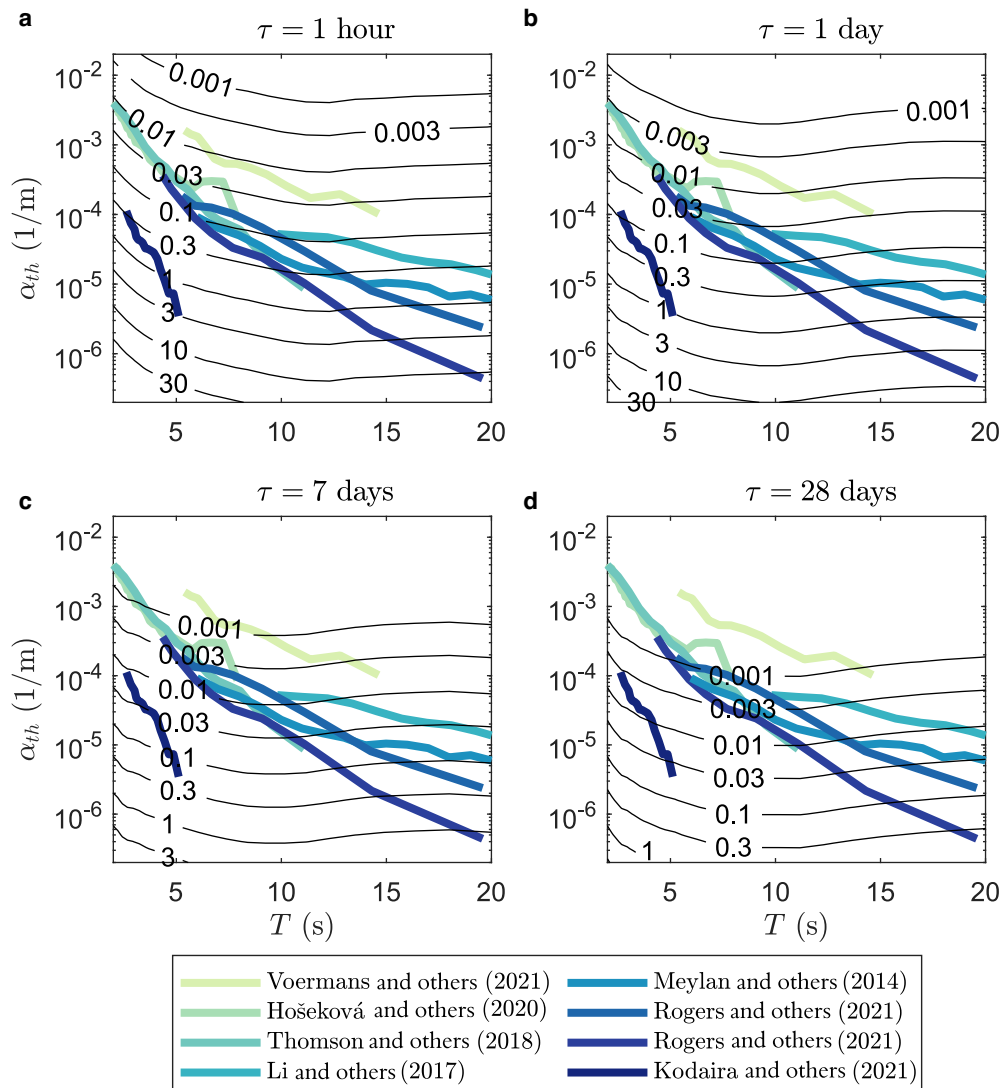


Fig. 2. The 95% confidence interval of the error $(\bar{\alpha} - \alpha_{th})/\alpha_{th}$ (contours) for averaging periods τ of (a) 1 h, (b) 1 d, (c) 7 d and (d) 28 d. Various field observations of α as a function of wave period T are shown in color.

The underlying problem of estimating α based on large t_0 is that it requires ice conditions to be similar in both temporal and spatial domains at the instants at which the observations

are obtained, which may significantly hinder the feasibility of such an approach. Nevertheless, to provide further insight into how the ice conditions may be treated numerically in the spatial

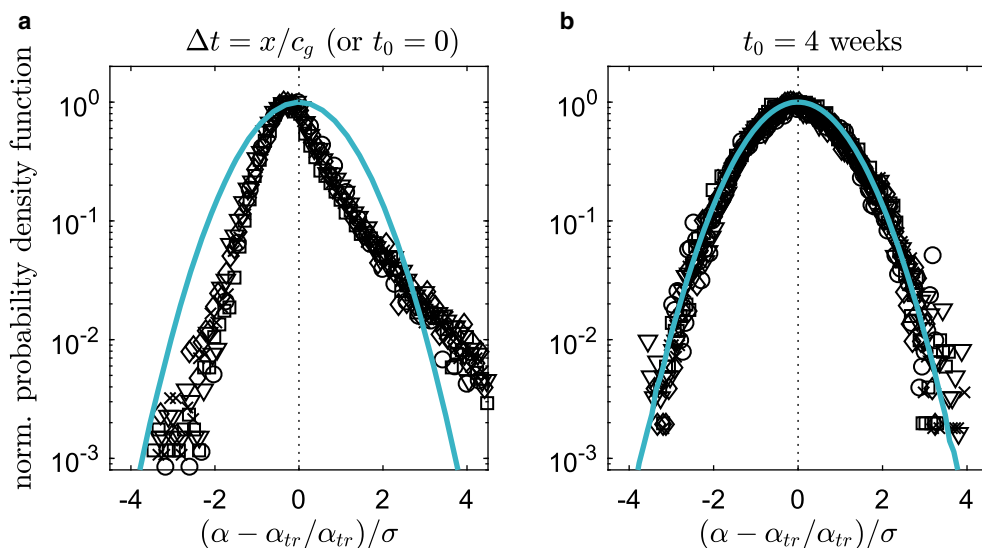


Fig. 3. Normalized probability density function of the error α , normalized by its standard deviation σ , for $T = 7.0$ s (circles), 8.4 s (triangles), 10.2 s (squares), 12.3 s (crosses) and 14.9 s (diamonds). Blue line is the best fit normal distribution, dash lines correspond to the mean of the data distributions.

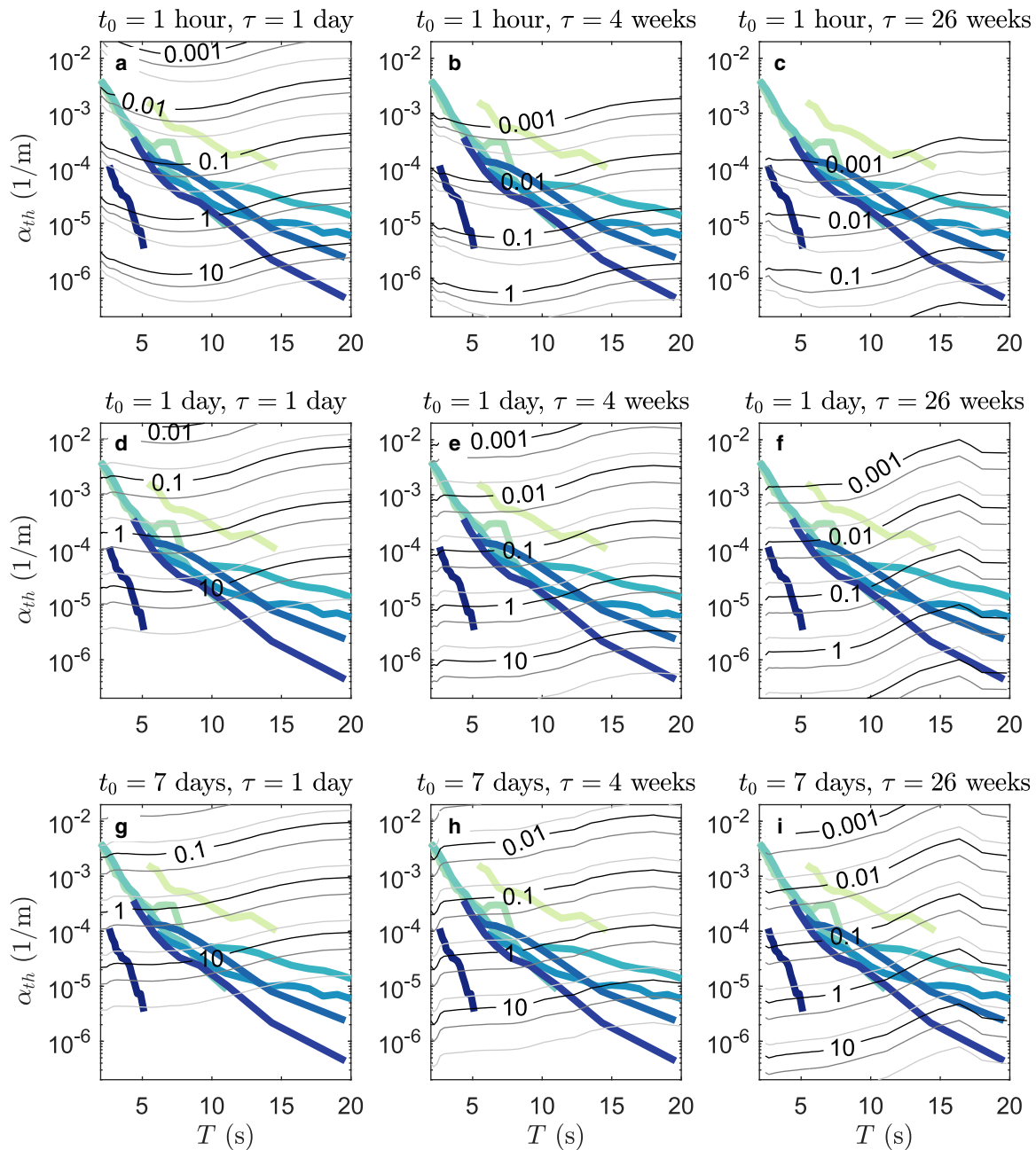


Fig. 4. The 95% confidence interval of the error $(\bar{\alpha} - \alpha_{th})/\alpha_{th}$ (contours) for various averaging periods τ and time offset between instrument measurements t_0 . Contour colors refer to the instrument separation distance x of 5, 10 and 30 km (black to light gray, respectively), with $x = 5$ km always being the largest error. Various field observations of α as a function of wave period T are shown in color, see Fig. 2 for legend.

domain in such a scenario, we look at an idealized case where sea-ice conditions are spatially inhomogeneous. For this we consider the case where α_{th} increases/decreases exponentially with distance x . By taking the simple case where $\Delta t = 0$, we infer that a simple spatial average of α between $x = 0$ and $x = x$ is a good approximation of the effective wave attenuation coefficient at x , with an error of $<5\%$ (we will refer to this spatial average value of α as $\langle \alpha \rangle$). The impact of the spatial heterogeneity of sea ice on the error of $\langle \alpha \rangle$ due to the assumption of wave stationarity is shown in Fig. 5, with the attenuation rate profiles shown in Figs 5a, d. We note that in our calculations x is now variable such that, in the example of $x = 100$ km and the attenuation profile given by Fig. 5a, α_{th} is 1×10^{-6} at $x = 0$ and 3.2×10^{-5} at $x = 100$ km, which leads to a spatially averaged attenuation rate of $\langle \alpha \rangle = 9 \times 10^{-6}$. In line with earlier observations that the error is largest in cases of low α_{th} (e.g. see Fig. 2), we observe here that the errors are initially large for an exponentially increasing

attenuation rate profile (Fig. 5b). However, such errors rapidly decrease when larger averaging periods are taken (see Fig. 5c where $\tau = 7$ d). Reversal of the attenuation rate profile leads to considerably larger values of $\langle \alpha \rangle$ and, consequently, shows that errors due to the adoption of the wave stationarity assumption are relatively small even for averaging periods of just 1 d (Fig. 5e). In Fig. 6 the same cases are considered, but now with a time offset of $t_0 = 7$ d. While the errors increase as one may expect, reasonable estimates of $\langle \alpha \rangle$ can still be obtained as long as $\langle \alpha \rangle$ is sufficiently large. This has useful implications for our modeling methods of waves in sea ice as the effective attenuation rate across an inhomogeneous ice cover can be approximated as spatial average of the local attenuation rate profile (and thus perhaps as the spatially weighted average of the ice types and ice features within such a domain), and the zero time offset $t_0 = 0$ is not necessarily a constraint to obtain reasonable estimates of $\langle \alpha \rangle$. Care should nevertheless be taken in applying

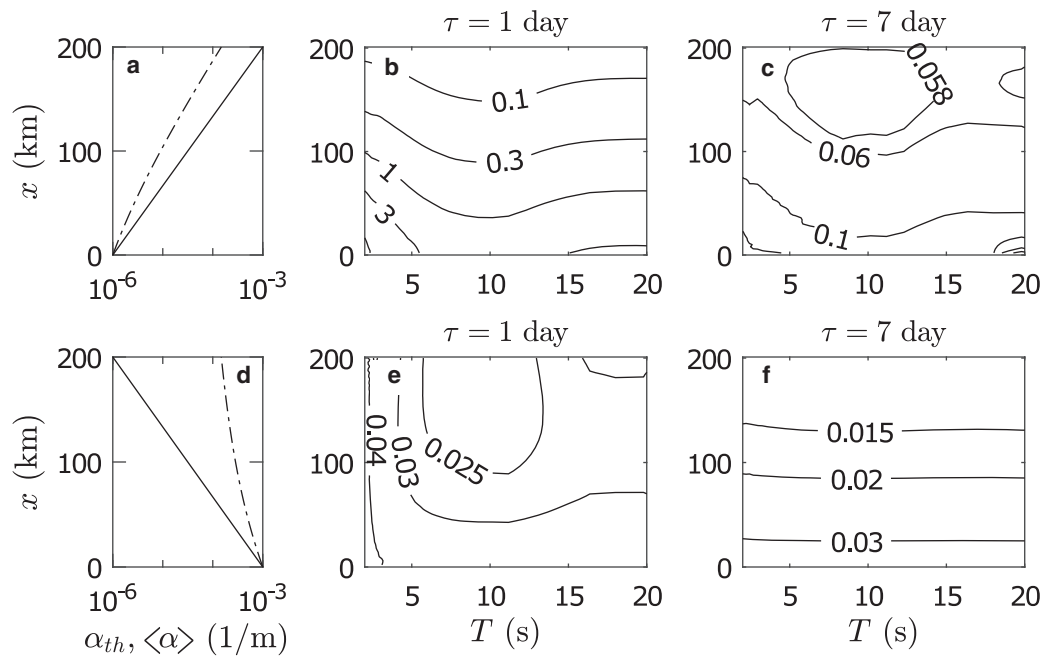


Fig. 5. The 95% confidence interval of the error $(\bar{\alpha} - \langle\alpha\rangle)/\langle\alpha\rangle$ for two spatially heterogeneous ice covers and $t_0 = 0$. The imposed spatial attenuation profiles are shown in (a) and (d), solid line, leading to errors in α as shown in (b, c) and (e, f) respectively, for different values of τ . The spatially averaged attenuation profile $\langle\alpha\rangle$, which is the cumulative effect of the local profile of α_{th} , is given in (a) and (d) by the dashed line.

such a simplified approach, as our understanding of wave attenuation and its relation to ice conditions remains very limited.

While this study can be used to inform past and future measurement campaigns on the errors and uncertainties in α associated with the stationarity assumption, we note that further research is required on the limitations of our analysis, and other potential methodological biases in estimating α from field observations. In particular, further study is required on the validity of Eqn (1) (e.g. Squire, 2018), as there is growing support α has a dependency on the local wave energy (Toffoli and others, 2015; Herman, 2021; Voermans and others, 2021). Other assumptions typically adopted in the estimation of α are related to the

directionality of the wave energy (e.g. Montiel and others, 2022), importance of wind-input, and non-linear wave-wave interactions. Lastly, we would like to point out that there are ways to avoid the adoption of the wave stationarity assumption altogether, such as by using model-data inversion (Rogers and others, 2021). Additionally, carefully designed field experiments could, in principle, take into consideration the propagation time of wave energy when estimating α . This can be the case when continuous time series of surface elevation are obtained (e.g. Sutherland and Rabault, 2016). However, this is, of course, far from straightforward task in the harsh and remote environments of the polar regions.

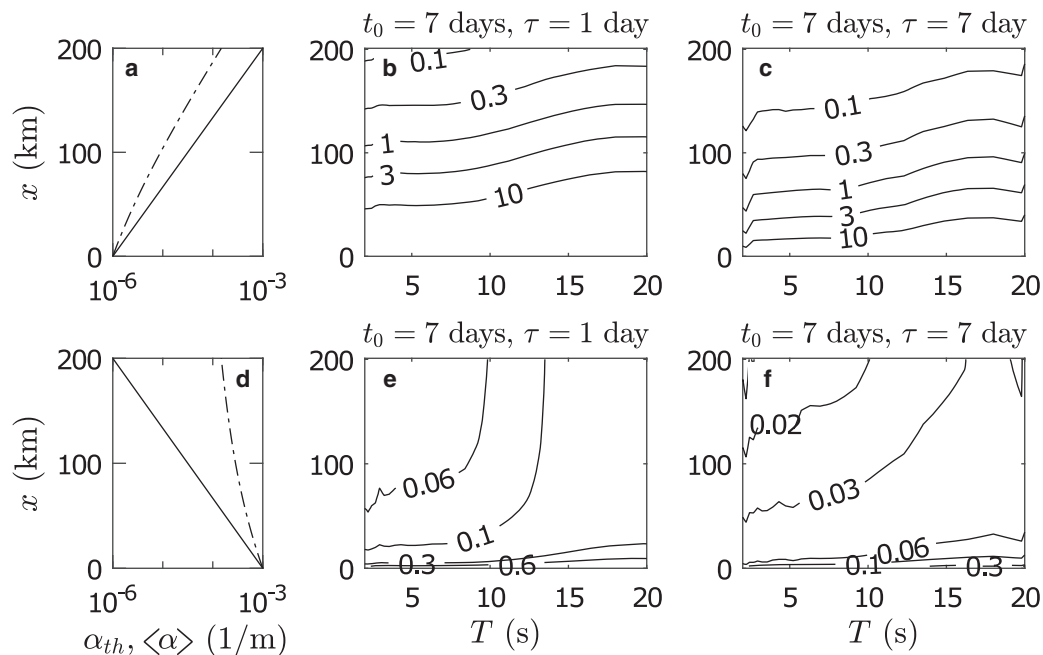


Fig. 6. Same as Fig. 5, but with $t_0 = 7$ d.

Concluding remarks

In this study the impact of the wave stationarity assumption on estimates of ice-induced wave energy attenuation is quantified. When wave attenuation rates are low, the apparent wave attenuation may become negative when the travel time of wave energy is not considered, and should thus not be interpreted a priori as erroneous data or wave growth. We observe that the wave stationarity assumption holds as long as the temporal averaging period is sufficiently long. The averaging period required to obtain accurate estimates of wave attenuation in the field increases with a decrease in the wave attenuation rate. Thus, for waves in unconsolidated sea ice, longer averaging periods are required in comparison with waves in consolidated or landfast ice. Surprisingly, even when wave conditions between two measurement points are measured as much as weeks apart, and thus the measured wave energy between the measurement points have become uncorrelated, good estimates of the wave attenuation coefficient can still be obtained provided that the averaging period of the measurements is sufficiently long. This provides significant opportunities in using satellite products with limited temporal resolution to estimate the wave attenuation rate at global scales. This thus may solve for one of the current problems in the field, namely, that observations of wave attenuation in sea ice are very limited and geographically sparse. Care should, however, be given in the way samples are averaged using this approach, as the overall ice conditions are required to remain constant across such measurement events. Such an approach may, however, still be feasible due to the vast amount of satellite observations currently available. Lastly, we observe that the spatial average of the attenuation rate of an inhomogeneous ice cover represents a good approximation of the effective wave attenuation rate, which may provide directions for the treatment of large scale sea-ice inhomogeneities in wave forecasting models and derivation of empirical ice classifications from satellite-derived sea-ice products.

Supplementary material. The supplementary material for this article can be found at <https://doi.org/10.1017/jog.2022.99>.

Acknowledgements. We acknowledge Sofar Ocean Technologies for the wave buoy deployment and providing wave buoy data, and the Copernicus Climate Change Service at ECMWF for making the ERA5 reanalysis data available. JJV and AVB acknowledge support from the Australian Antarctic Program under project 4593. AVB acknowledges support from the US Office of Naval Research (grant N62909-20-1-2080). The authors thank the two anonymous reviewers for their comments and suggestions which significantly improved this manuscript.

Author contributions. JJV: conceptualization, methodology, analysis, writing – original draft. XX: methodology, analysis, writing – review and editing. AVB: supervision, writing – review and editing.

References

- Brouwer J and 9 others (2022) Altimetric observation of wave attenuation through the Antarctic marginal ice zone using ICESat-2. *The Cryosphere* **16**(6), 2325–2353.
- Cheng S and 9 others (2017) Calibrating a viscoelastic sea ice model for wave propagation in the Arctic fall marginal ice zone. *Journal of Geophysical Research: Oceans* **122**(11), 8770–8793.
- Herman A (2021) Spectral wave energy dissipation due to under-ice turbulence. *Journal of Physical Oceanography* **51**(4), 1177–1186.
- Herman A, Cheng S and Shen HH (2019) Wave energy attenuation in fields of colliding ice floes – part 2: a laboratory case study. *The Cryosphere* **13**(11), 2901–2914.
- Horvat C, Blanchard-Wrigglesworth E and Petty A (2020) Observing waves in sea ice with ICESat-2. *Geophysical Research Letters* **47**(10), e2020GL087629.
- Hošeková L and 7 others (2020) Attenuation of ocean surface waves in pancake and frazil sea ice along the coast of the Chukchi Sea. *Journal of Geophysical Research: Oceans* **125**(12), e2020JC016746.
- Kodaira T and 6 others (2021) Observation of on-ice wind waves under grease ice in the Western Arctic Ocean. *Polar Science* **27**, 100567.
- Kohout AL and Meylan MH (2008) An elastic plate model for wave attenuation and ice floe breaking in the marginal ice zone. *Journal of Geophysical Research: Oceans* **113**(C9), C09016.
- Kohout AL, Meylan MH and Plew DR (2011) Wave attenuation in a marginal ice zone due to the bottom roughness of ice floes. *Annals of Glaciology* **52**(57), 118–122.
- Li J and 5 others (2017) Rollover of apparent wave attenuation in ice covered seas. *Journal of Geophysical Research: Oceans* **122**(11), 8557–8566.
- Løken TK, Ellevold TJ, de la Torre RGR, Rabault J and Jensen A (2021) Bringing optical fluid motion analysis to the field: a methodology using an open source ROV as a camera system and rising bubbles as tracers. *Measurement Science and Technology* **32**(9), 095302.
- Meylan MH, Bennetts LG and Kohout AL (2014) In situ measurements and analysis of ocean waves in the Antarctic marginal ice zone. *Geophysical Research Letters* **41**(14), 5046–5051.
- Montiel F, Kohout AL and Roach LA (2022) Physical drivers of ocean wave attenuation in the marginal ice zone. *Journal of Physical Oceanography* **52**(5), 889–906.
- Montiel F, Squire V and Bennetts L (2016) Attenuation and directional spreading of ocean wave spectra in the marginal ice zone. *Journal of Fluid Mechanics* **790**, 492–522.
- Nelli F, Bennetts LG, Skene DM and Toffoli A (2020) Water wave transmission and energy dissipation by a floating plate in the presence of overwash. *Journal of Fluid Mechanics* **889**, 75.
- Rabault J and 9 others (2022) Openmetbuoy-v2021: an easy-to-build, affordable, customizable, open-source instrument for oceanographic measurements of drift and waves in sea ice and the open ocean. *Geosciences* **12**(3), 110.
- Rabault J, Sutherland G, Jensen A, Christensen KH and Marchenko A (2019) Experiments on wave propagation in grease ice: combined wave gauges and particle image velocimetry measurements. *Journal of Fluid Mechanics* **864**, 876–898.
- Rogers WE, Meylan MH and Kohout AL (2021) Estimates of spectral wave attenuation in Antarctic Sea ice, using model/data inversion. *Cold Regions Science and Technology* **182**, 103198.
- Shen HH (2019) Modelling ocean waves in ice-covered seas. *Applied Ocean Research* **83**, 30–36.
- Squire VA (2018) A fresh look at how ocean waves and sea ice interact. *Philosophical Transactions of the Royal Society A: Mathematical, Physical and Engineering Sciences* **376**(2129), 20170342.
- Squire VA (2020) Ocean wave interactions with sea ice: a reappraisal. *Annual Review of Fluid Mechanics* **52**, 37–60.
- Squire VA and Allan AJ (1980) Propagation of flexural gravity waves in sea ice. *Proceedings of the Arctic Ice Dynamics Joint Experiment*. Seattle: University of Washington Press, pp. 327–338.
- Sree DK, Law AWK and Shen HH (2018) An experimental study on gravity waves through a floating viscoelastic cover. *Cold Regions Science and Technology* **155**, 289–299.
- Stopa JE, Ardhuin F and Girard-Ardhuin F (2016) Wave climate in the Arctic 1992–2014: seasonality and trends. *The Cryosphere* **10**(4), 1605–1629.
- Sutherland G and Rabault J (2016) Observations of wave dispersion and attenuation in landfast ice. *Journal of Geophysical Research: Oceans* **121**(3), 1984–1997.
- Sutherland G, Rabault J, Christensen KH and Jensen A (2019) A two layer model for wave dissipation in sea ice. *Applied Ocean Research* **88**, 111–118.
- Thomson J and 10 others (2018) Overview of the Arctic Sea state and boundary layer physics program. *Journal of Geophysical Research: Oceans* **123**(12), 8674–8687.
- Thomson J, Hošeková L, Meylan MH, Kohout AL and Kumar N (2021) Spurious rollover of wave attenuation rates in sea ice caused by noise in field measurements. *Journal of Geophysical Research: Oceans* **126**(3), e2020JC016606.
- Toffoli A and 6 others (2015) Sea ice floes dissipate the energy of steep ocean waves. *Geophysical Research Letters* **42**(20), 8547–8554.
- Voermans JJ and 9 others (2020) Experimental evidence for a universal threshold characterizing wave-induced sea ice break-up. *The Cryosphere* **14**(11), 4265–4278.
- Voermans JJ and 9 others (2021) Wave dispersion and dissipation in landfast ice: comparison of observations against models. *The Cryosphere* **15**(12), 5557–5575.

- Voermans J, Babanin A, Thomson J, Smith M and Shen H** (2019) Wave attenuation by sea ice turbulence. *Geophysical Research Letters* **46**(12), 6796–6803.
- Wadhams P, Squire VA, Goodman DJ, Cowan AM and Moore SC** (1988) The attenuation rates of ocean waves in the marginal ice zone. *Journal of Geophysical Research: Oceans* **93**(C6), 6799–6818.
- Wang R and Shen HH** (2010) Gravity waves propagating into an ice-covered ocean: a viscoelastic model. *Journal of Geophysical Research: Oceans* **115**(C6), C06024.
- Weber JE** (1987) Wave attenuation and wave drift in the marginal ice zone. *Journal of Physical Oceanography* **17**(12), 2351–2361.